Acta Pharmaceutica Sinica B 2018;8(4):645–654

Chinese Pharmaceutical Association
Institute of Materia Medica, Chinese Academy of Medical Sciences

Acta Pharmaceutica Sinica B

www.elsevier.com/locate/apsb
www.sciencedirect.com

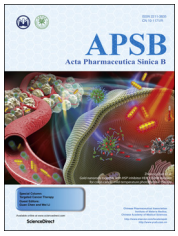

ORIGINAL ARTICLE

Authentic compound-free strategy for simultaneous determination of primary coumarins in Peucedani Radix using offline high performance liquid chromatography–nuclear magnetic resonance spectroscopy–tandem mass spectrometry

Yao Liu[a], Qingqing Song[a], Wenjing Liu[a], Peng Li[b], Jun Li[a], Yunfang Zhao[a], Liang Zhang[c], Pengfei Tu[a], Yitao Wang[b,*], Yuelin Song[a,*]

[a]*Modern Research Center for Traditional Chinese Medicine, School of Chinese Materia Medica, Beijing University of Chinese Medicine, Beijing 100029, China*
[b]*State Key Laboratory of Quality Research in Chinese Medicine, Institute of Chinese Medical Sciences, University of Macau, Taipa 999078, Macao, China*
[c]*State Key Laboratory of Tea Plant Biology and Utilization, Anhui Agricultural University, Hefei 230036, China*

Received 5 October 2017; received in revised form 25 November 2017; accepted 12 December 2017

KEY WORDS

Authentic compound-independent quantitation;
Offline LC–NMR–MS/MS;
Automated fraction collection module;
Quantitative ^{1}H NMR;
Peucedani Radix;
Regio-specific monitoring

Abstract Herein, a strategy is proposed for the simultaneous determination of primary coumarins in Peucedani Radix (Chinese name: Qianhu). The methodology consists of three consecutive steps: 1) Semi-preparative LC in combination with a home-made automated fraction collection module to fragment the universal metabolome standard into ten fractions (Frs. I–X); 2) LC–accurate MS/MS and quantitative ^{1}H NMR spectroscopy conducted in parallel to acquire the qualitative and quantitative data of each fraction; 3) Robust identification and quantification of components by use of LC coupled to multiple reaction monitoring. In this final step, the most significant fractions (Frs. III–X) were pooled to serve as the pseudo-mixed standard solution. Meticulous online parameter optimization was performed to obtain the optimal parameters, including ion transitions and collision energies. Concerns were particularly paid onto pursuing the parameters being capable of monitoring *regio*-

*Corresponding authors.
E-mail addresses: ytwang@umac.mo (Yitao Wang), syltwc2005@163.com (Yuelin Song).

Peer review under responsibility of Institute of Materia Medica, Chinese Academy of Medical Sciences and Chinese Pharmaceutical Association.

https://doi.org/10.1016/j.apsb.2018.01.005

specific isomers, notably praeruptorin E *vs.* 3′-isovaleryl-4′-angeloylkhellactone. The quantitative performance of the method was validated according to diverse assays. Eleven primary coumarins (**1**–**11**) were unambiguously identified and absolutely quantified, even though no external reference compound was used. Above all, the integrated strategy not only provides a feasible pipeline for the quality assessment of Peucedani Radix, but more importantly, shows the potential for authentic compound-free quantitative evaluation of traditional Chinese medicines.

1. Introduction

Traditional Chinese medicines (TCMs) have played determinant roles in the health of Chinese people over the past centuries because of their cogent therapeutic benefits[1]. Recently, TCMs are drawing global attention because their unique system-to-system effective principle matches well with chronic diseases as well as those multi-factorial disorders[2,3]. To guarantee the safety and efficacy of TCMs in clinical use, it is important to conduct strict quality control analyses for crude materials, mainly herbal medicines[4,5]. High performance liquid chromatography (LC), in particular coupled online with tandem mass spectrometry (MS/MS), is serving as a workhorse for quality analyses of TCMs Owing to the advantages of sensitivity, specificity, and high throughput. However, the bottleneck subsequently comes over the availability and/or high cost of authentic compounds to serve as external standards which are mandatory for reliably transforming peak areas into absolute concentrations of analytes. Although the quantitative analysis of multi-components by single marker (QAMS)[6] or single standard to determine multi-components (SSDMC)[6,7] has been claimed as a robust methodology to cope with the shortage of reference standards[8], authentic substances are still needed to obtain the relative response factors (*i.e.* conversion factors) between each analyte and the "single marker" in each laboratory. Herein, we attempt to circumvent even the demand of the "single marker" for the quality control of TCMs.

Among the approaches to absolute quantitation without the use of authentic compounds, quantitative ^{1}H NMR (q^1H NMR) has been widely favored as an integral part of the analytical chemist's toolbox. Because the resonance signal is theoretically, directly proportional to the number of resonant nuclei, the requirement for the reference substance for each analyte can be bypassed by employing an easily available as well as cheap compound as the internal standard (IS) for q^1H NMR[8,9]. However, NMR is disadvantageous, intrinsically, at sensitivity as well as resolution, thus leading to a technical barrier for directly applying q^1H NMR for simultaneous determination of dozens of analytes-of-interest in TCMs that has been widely claimed as complicated compound pools.

The most straightforward scheme to combine the merits of LC, MS/MS, and NMR is purification of analytes with LC, structural identification with NMR, and quantitation with LC–MS/MS, successively. However, this approach is extremely time-consuming and laborious. More recently, it has now become possible to extract exact quantitative and qualitative information from ^{1}H NMR spectrum of a relative simple mixture of a dozen compounds by use of NMR along with of various databases, *e.g.* HMDB[10] and COLMARm[11]. Therefore, fractionation (*vs.* complete purification) is more feasible to bridge the gap between NMR and LC–MS/MS. We herein propose a practical strategy consisting of three consecutive steps: 1) fragmenting crude herbal extracts into ten fractions using semi-preparative LC equipped with a home-made automated fraction collection module; 2) acquiring the qualitative as well as quantitative information of each fraction by parallel measurements with LC–accurate MS/MS and q^1H NMR spectroscopy; and 3) pooling the relevant fractions to serve as pseudo-mixed standard solution for simultaneous determination of the primary components using LC–MS/MS.

As a proof of concept, multi-component targeted quantitation of Peucedani Radix (Chinese name: Qianhu) which is derived from the dried roots of *Peucedanum praeruptorum* DUNN was conducted in current study[12]. The herbal medicine is rich of angular-type pyranocoumarins (APs)[13–18], and its therapeutic benefits such as coronary diastole[19], anti-hypertension[20], and myocardial protection[21] have been well defined. Moreover, we also aimed to assess the potential of MS/MS towards advancing the chromatographic separation of LC, because Peucedani Radix is rich in positional isomers, *e.g.* pteryxin (Pte) *vs.* praeruptorin A (PA)[14] and praeruptorin E (PE) *vs.* 3′-isovaleryl-4′-angeloylkhellactone (IAK)[22], and chromatographic overlapping peaks, even co-elution, widely occurs in LC analyses of these mixtures. These findings can establish the new strategy as a robust, authentic, compound-free approach for the quality assessment of Peucedani Radix as well as other TCMs.

2. Experimental

2.1. Chemical and materials

Formic acid, methanol, and acetonitrile (ACN) were of LC–MS grade and purchased from Thermo-Fisher (Pittsburgh, PA, USA). Deionized water was prepared in-lab using a Milli-Q purification instrument (Millipore, Bedford, MA, USA). $CDCl_3$ (deuterium abundance, 99.96 atom% deuterium) was purchased from Cambridge Isotope Laboratories Inc. (Miami, FL, USA). Analytical grade methanol was supplied by Xilong Scientific (Shantou, Guangdong, China). Pyrazine (purity > 99%) that served as IS1 for q^1H NMR was obtained from Aldrich (St Louis, MO, USA). 1,2,3,7-Tetramethoxyxanthone which served as IS2 for LC–MS/MS-based quantitation, was obtained from the chemical library of the State Key Laboratory of Natural and Biomimetic Drugs, Peking University (Beijing, China).

Eleven batches of pulverized Peucedani Radix (PR1–11) as well as universal metabolome standard (UMS) described in our previous article[14] were introduced in current study.

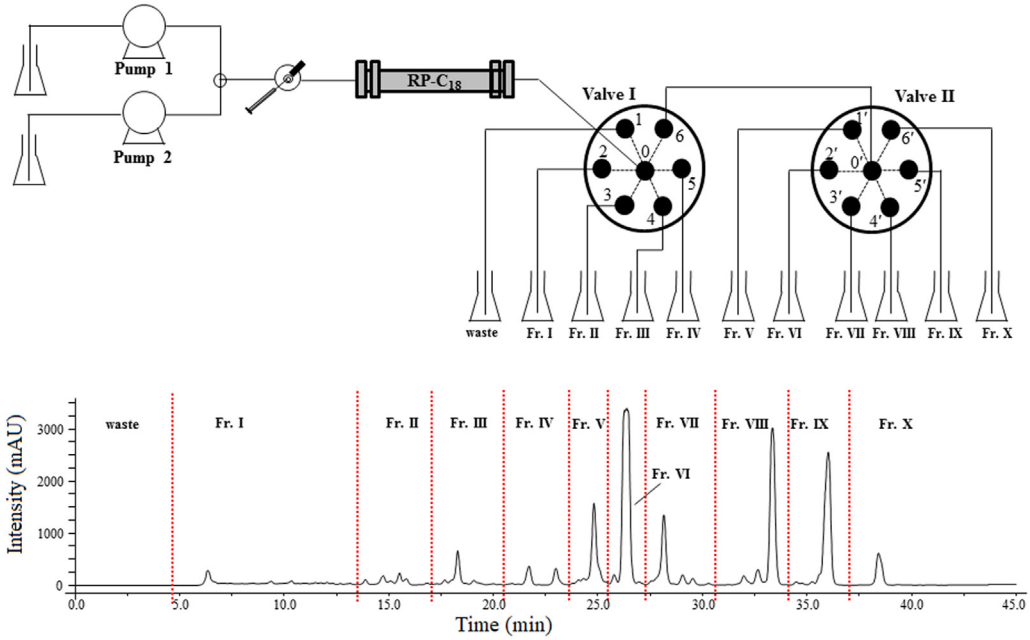

Figure 1 (A) Connectivity sketch of the home-made automated fraction collection module consisting of two 7-port/6-channel electronic valves (Valves I and II). (B) Representative chromatogram of UMS obtained from semi-preparative LC and the collection program is also illustrated.

2.2. *Fractionation of UMS using semi-preparative LC equipped with automated fraction collection module*

The UMS sample was chromatographed on a Shimadzu LC-20AT modular system (Kyoto, Japan) composed of two LC-20AT pumps, a DGU-20A_{3R} degasser, a SPD-M20A DAD module, and a CBM-20A controller. A YMC-Pack C_{18} column (250 mm × 10 mm, 5 μm, Kyoto, Japan) was used for chromatographic separations. The mobile phase consisted of water (A) and methanol (B), and the gradient elution was programed as follows: 0–5.0 min, 50%–70%B; 5.0–10.0 min, 70%–75%B; 10.0–25.0 min, 75–85%B; 25.0–37.0 min, 85%–95%B; 37.0–37.1 min, 95%–50%B; 37.1–45.0 min, 50%B; and flow rate, 2.0 mL/min. UV length of DAD module was monitored at 320 nm. An automated fraction collection module was configured by employing two 7-port/6-channel electronic valves (Fig. 1A) as well as some necessary PEEK tubing (i.d. 0.13 mm), and ten fractions (Frs. I–X), corresponding to the effluents among 4.0–13.5, 13.5–16.5, 16.5–21.0, 21.0–24.0, 24.0–25.8, 25.8–27.5, 27.5–31.5, 31.5–34.5, 34.5–38.0, and 38.0–45.0 min, were automatically collected through an optimized channel switching program for both valves (Fig. 1B), whereas the 0–4.0 min portion was introduced into the waste. The UMS sample yielded from 1.0 g of pooled crude material were subjected to chromatographic fractionation.

2.3. *Parallel measurements of all fractions using NMR and LC–accurate MS/MS*

After the removal of a 50 μL aliquot, each fraction underwent lyophilization and the residues were individually reconstituted with 600 μL of $CDCl_3$ containing 0.37 mmol/L IS1. After thorough dissolution, the resultant solution was transferred into a NMR tube (i.d. 5 mm, Norell ST500-7, Morganton, NC, USA) for NMR assays. The minor portion (50 μL) of each fraction was injected into the LC–accurate MS/MS system *via* the auto-sampler.

q^{1}H NMR was conducted on a Varian UNITY plus 500 MHz spectrometer (VNMR500, Varian Inc., Palo Alto, CA, USA) at 499.91 MHz proton frequency equipped with TCI cryoprobe and *Z*-gradient system, and those default settings were applied for all spectral acquisition. LC–accurate MS/MS measurements were conducted on a Shimadzu LC–IT-TOF-MS platform[14]. A CAPCELL CORE C18 column (150 mm × 2.1 mm, 2.7 μm, Shiseido, Kyoto, Japan) was used for chromatographic separations, and gradient elution was programmed as described in our previous article[16]. The UV absorbance was monitored at 190–400 nm. The column was maintained at 40 °C and an injection volume of 5.0 μL was used.

2.4. *Regio-specific monitoring of positional isomers*

After that unambiguous identities were transmitted from jointly analyzing LC–IT-TOF-MS and NMR spectroscopic datasets (Supplemental Information Figs. S1–10), those components including qianhucoumarin D (**1**)[23], 3′-angeloyloxy-4′-oxo-3′,4′-dihydroseselin (**2**)[15], 3′-isovaleryloxy-4′-oxo-3′,4′-dihydroseselin (**3**)[24], Pte (**4**)[15], PA (**5**)[15], *cis*-3′-isovaleryl-4′-acetylkhellactone (**6**)[15], imperatorin (**7**)[25], praeruptorin B (**8**)[15], IAK (**9**)[22], PE (**10**)[15], and *cis*-3′,4′-*di*-isovalerylhellactone (**11**)[15] (Fig. 2, and Table 1), eleven coumarins in total, were selected as analytes. A hybrid triple quadrupole-linear ion trap mass spectrometer (Qtrap-MS, Sciex5500, Foster City, CA, USA) equipped with a Turbo V^{TM} ESI interface was then employed for quantitative measurement, and the settings for LC domain[16] and the ion-source parameters[14] was identical with previous descriptions.

Except for two pairs of positional isomers (Pte *vs.* PA and PE *vs.* IAK), the optimal parameters of other analytes, such as collision energy (CE), declustering potential (DP), and precursor-to-product ion transitions for multiple reaction monitoring (MRM), followed the values described in our previous studies (Supplemental Information Table S1)[14,16]. Because significantly overlapping signals were observed between PE and AIK, exclusive parameters were required for either *regio*-isomer. To assist the screening of parameters with satisfactory specificity, another pair

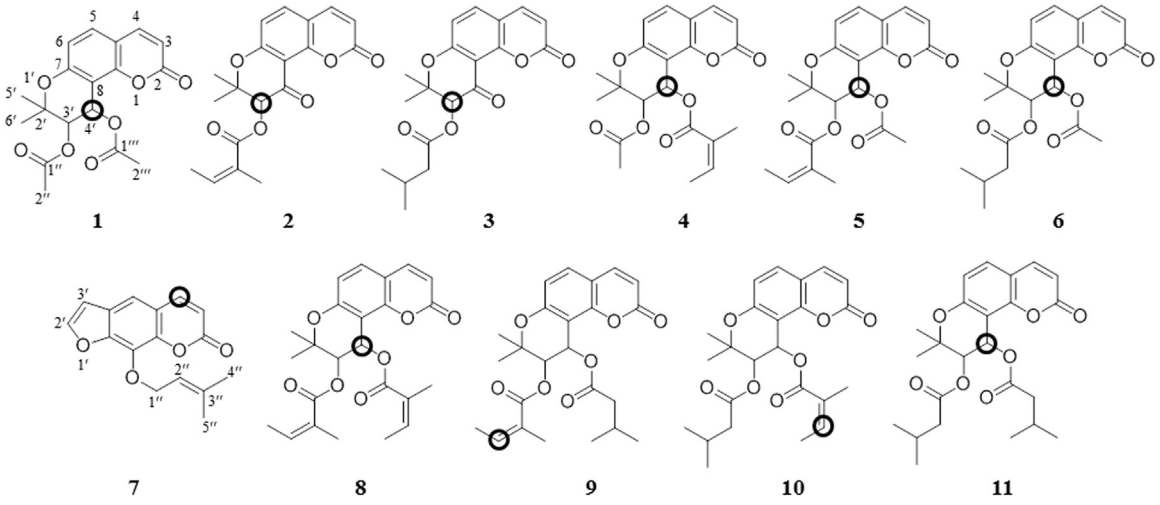

Figure 2 Chemical structures for all compounds-of-interest (**1–11**). The protons indicated with circles are chosen as quantitative signals.

of positional isomers namely Pte and PA, were also included for careful online parameter optimization[14,26], because the isomeric pattern between Pte and PA was identical with that of PE *vs.* AIK and satisfactory separation was accomplished for Pte and PA. Diverse ion transition candidates were assayed, *i.e. m/z* 409 > 349, 409 > 327, 409 > 309, 409 > 287, 409 > 245, 409 > 227, 404 > 344, 404 > 327, 404 > 304, 404 > 287, 404 > 245, 404 > 227, 387 > 327, 387 > 287, 387 > 245, 387 > 227, 327 > 245, 327 > 227, 327 > 215, 287 > 245, 287 > 227, and 287 > 215 for either Pte or PA, and 451 > 351, 451 > 349, 451 > 329, 451 > 327, 451 > 245, 451 > 227, 446 > 346, 446 > 344, 446 > 329, 446 > 327, 446 > 245, 446 > 227, 429 > 329, 429 > 327, 429 > 245, 429 > 227, 329 > 245, 329 > 227, 329 > 215, 327 > 245, 327 > 227, and 327 > 215 for either PE or IAK. CEs ranged from 5 to 60 eV were stepwise screened (step-size: 1 eV) for each ion transition candidate.

2.5. *Method validation and simultaneous determination*

The concentration of each targeted compound was calculated from q^{1}H NMR spectroscopy by applying the published equation[15,27]. Except for Frs. I and II, Frs. III–X were then thoroughly pooled, dried, and reconstituted with methanol, successively, to generate the pseudo-mixed standard solution with concentration profile as 87.50, 67.50, 7.50, 178.75, 1505.00, 240.00, 18.75, 490.00, 100.50, 435.00, and 138.75 μg/mL for compounds **1–11**, sequentially. The pseudo-mixed standard solution was then serially diluted with methanol to yield a set of working standard samples. Subsequently, those samples were 2-fold diluted with methanol containing 500 ng/mL of IS2 to create the new series of calibration samples. Diverse method validation assays, such as linearity, sensitivity, precision, recovery, stability, and matrix effect, were conducted by following the protocols described in the literature[14], and the role of UMS was replaced by selected working standard sample regarding linearity, sensitivity, precision, recovery, and matrix effect assays.

Sample extracts were prepared by thoroughly suspending pulverized materials (100 mg) in 10 mL of methanol and subjected to ultranonic extraction. After adding methanol to compensate for the lost weight during extraction, each extract was centrifuged at 10,000× *g* for 10 min and the supernatants were filtered through a 0.22 μm membrane. In parallel with those calibration samples, each filtrate was further 2-fold diluted with 500 ng/mL of IS2 fortified methanol prior to measurement. The validated method was then applied for simultaneous determination of eleven coumarins (**1–11**, Table 1) in all Peucedani Radix extracts (PR1–11).

3. Results and discussion

3.1. *Definitely structural identification by joint LC–IT-TOF-MS and NMR*

Due to the complexity of chemical constituents and the structural similarity among APs, it was virtually impossible to exactly assign the signals in ^{1}H NMR spectrum of the crude extract. Hence, fractionation was first performed on the extract. Several signals were prominent in UV (320 nm) chromatogram of UMS and these signals were thereby adopted as the landmarks to fragment the entire effluent into ten fractions (Frs. I–X) according to valve switching at 4.0, 13.5, 16.5, 21.0, 24.0, 25.8, 27.5, 31.5, 34.5, and 38.0 min, sequentially (Fig. 1B). The careful application of the NMR spectroscopic datasets to the LC–IT-TOF-MS data permitted definitive identification of a total of eleven coumarins (Fig. 2). Detailed information for each analyte is summarized in Table 1.

Herein, we selected Fr. IX as the representative one to describe the assignment of LC–IT-TOF-MS and NMR spectroscopic signals. Obviously, only one primary signal was observed when the UV length was maintained at 320 nm (Fig. 3A), and IT-TOF-MS afforded a series of signals, such as *m/z* 467 $[M + K]^+$, 451 $[M + Na]^+$, and 446 $[M + NH_4]^+$ in MS^1 spectrum (Fig. 3B), and *m/z* 351 $[M + Na - C_5H_8O_2]^+$, 349 $[M + Na - C_5H_{10}O_2]^+$, 327 $[M + H - C_5H_{10}O_2]^+$, 245 $[M + H - C_{10}H_{16}O_3]^+$, 227 $[M + H - C_{10}H_{18}O_4]^+$, and 215 $[M + H - C_{11}H_{18}O_4]^+$ in the MS^2 spectrum of *m/z* 451 (Fig. 3C). After matching those data with previous report[28], this primary peak was tentatively identified as PE, and the distribution of PE was also demonstrated by ^{1}H NMR spectroscopy *via* a set of signals (Table 1). However, a set of obvious signals that could not be assigned to PE were observed at δ 6.03, 2.00, and 1.88 in ^{1}H NMR spectrum. In combination of the chromatogram and tandem mass spectral profiles, the occurrence of AIK[22], a positional isomer of PE was unambiguously demonstrated in this fraction.

Table 1 Assignments of mass spectral and ^{1}H NMR ($CDCl_3$, 500 MHz) signals for eleven analytes in Frs. III–X.

Source	t_R[a] (min)	MS[1]	Molecular formula	MS[2]	^{1}H-NMR (δ in ppm, J in Hz)[b]	Identity
Fr. III	17.58	385.0679 $[M+K]^+$ 369.0926 $[M+Na]^+$ 364.1434 $[M+NH_4]^+$	$C_{19}H_{20}O_6$	309; 245; 227	6.25 (1H, d, J = 9.43 Hz, 3-H), 7.60 (1H, d, J = 9.41 Hz, 4-H), 7.34 (1H, d, J = 8.63, 5-H), 6.81 (1H, d, J = 8.43 Hz, 6-H), 5.34 (1H, d, J = 5.08 Hz, 3′-H), **6.53 (1H, d, J = 5.08 Hz, 4′-H)**, 1.41(3H, s, 5′-CH_3), 1.45 (3H, s, 6′-CH_3), 2.13 (3H, s, 2′′-CH_3), 2.10 (3H, s, 2′′′-CH_3)	Qianhucoumarin D (**1**)
Fr. IV	21.15	365.0996 $[M+Na]^+$ 360.1453 $[M+NH_4]^+$ 343.1204 $[M+H]^+$	$C_{19}H_{18}O_6$	265; 243	6.33 (1H, d, J = 9.59 Hz, 3-H), 7.59 (1H, d, J = 9.28 Hz, 4-H), 7.55 (1H, 5-H), 6.86 (1H, d, J = 8.53 Hz, 6-H), **5.67 (1H, s, 3′-H)**, 1.42 (3H, s, 5′-CH_3), 1.60 (3H, s, 6′-CH_3), 6.22 (1H, q, J = 6.58 Hz, 3′′-H), 2.04 (3H, d, J = 6.90 Hz, 4′′-CH_3), 1.98 (3H, s, 5′′-CH_3)	3′-Angeloyloxy-4′-oxo-3′,4′-dihydroseselin (**2**)
	22.54	383.0908 $[M+K]^+$ 367.1115 $[M+Na]^+$ 362.1633 $[M+NH_4]^+$	$C_{19}H_{20}O_6$	265; 243	6.36 (1H, d, J = 9.59 Hz, 3-H), 7.75 (1H, d, J = 9.81 Hz, 4-H), 6.87 (1H, d, J =8.34 Hz, 6-H), 7.53 (1H, 5-H), **5.57 (1H, s, 3′-H)**, 1.71 (3H, s, 5′-CH_3), 1.74 (3H, s, 6′-CH_3), 2.31 (1H, m, 2′′-H)	3′-Isovaleryloxy-4′-oxo-3′,4′-dihydroseselin (**3**)
Fr. V	24.25	425.101 $[M+K]^+$ 409.1335 $[M+Na]^+$ 404.1763 $[M+NH_4]^+$	$C_{21}H_{22}O_{77}$	327; 309; 287; 245; 227; 215	6.23 (1H, d, J = 9.48 Hz, 3-H), 7.59 (1H, d, J = 9.45 Hz, 4-H), 7.34 (1H, d, J = 8.44 Hz, 5-H), 6.79 (1H, d, J = 8.82 Hz, 6-H), 5.35 (1H, d, J = 4.92 Hz, 3′-H), **6.63 (1H, d, J = 4.90 Hz, 4′-H)**, 1.43 (3H, s, 5′-CH_3), 1.46 (3H, s, 6′-CH_3), 2.09(1H, s, 3′′-CH_3), 6.04 (1H, q, J = 6.69 Hz, 3′′′-H), 2.01 (3H, d, J = 6.50 Hz, 4′′′-CH_3), 1.86 (3H, s, 5′′′-CH_3)	Pte (**4**)
Fr. VI	25.79	425.0852 $[M+K]^+$ 409.1269 $[M+Na]^+$ 404.1736 $[M+NH_4]^+$	$C_{21}H_{22}O_7$	349; 327; 309; 245; 227; 215	6.24 (1H, d, J = 9.55 Hz, 3-H), 7.58 (1H, d, J = 9.46 Hz, 4-H), 7.33 (1H, d, J = 8.76 Hz, 5-H), 6.81 (1H, d, J = 8.66 Hz, 6-H), 5.41(1H, d, J = 4.89 Hz, 3′-H), **6.58 (1H, d, J = 4.80 Hz, 4′-H)**, 1.43 (3H, s, 5′-CH_3), 1.47 (3H, s, 6′-CH_3), 6.13 (1H, q, J = 6.95 Hz, 3′′-H), 1.96 (3H, d, J = 6.88 Hz, 4′′′-CH_3), 1.86 (3H, s, 5′′-CH_3), 2.10 (3H, s, 2′′′-CH_3)	PA (**5**)
Fr. VII	27.64	427.1219 $[M+K]^+$ 411.1405 $[M+Na]^+$ 406.1864 $[M+NH_4]^+$	$C_{21}H_{24}O_7$	351; 329; 327; 245; 215	6.24 (1H, d, J = 9.53 Hz, 3-H), 7.60 (1H, d, J = 9.49 Hz, 4-H), 7.33 (1H, d, J = 8.56 Hz, 5-H), 6.80 (1H, d, J = 8.61 Hz, 6-H), 5.33 (1H, d, J = 4.85 Hz, 3′-H), **6.54 (1H, d, J = 4.89 Hz, 4′-H)**, 1.40 (3H, s, 5′-CH_3), 1.44 (3H, s, 6′-CH_3), 0.99 (6H, d, J = 6.93, 4′′, 5′′-CH_3), 2.13 (3H, s, 2′′′-CH_3)	*cis*-3′-Isovaleryl-4′-acetylkhellactone (**6**)
	28.83	309.0543 $[M+K]^+$ 293.0795 $[M+Na]^+$ 271.0959 $[M+H]^+$	$C_{16}H_{14}O_6$	225; 203	6.26 (1H, d, J = 9.82 Hz, 3-H), **8.15 (1H, d, J = 9.72 Hz, 4-H)**, 7.05 (1H, s, 5-H), 6.95 (1H, d, J = 1.98 Hz, 2′-H), 7.60 (1H, 3′-H), 4.91 (1H, d, J = 7.38 Hz, 1′′-H), 5.54 (1H, t, J = 6.94 Hz, 2′′-H), 1.70 (3H, s, 4′′-CH_3), 1.80 (3H, s, 5′′-CH_3)	Imperatorin (**7**)
Fr. VIII	32.86	465.1277 $[M+K]^+$ 449.1585 $[M+Na]^+$ 444.2038 $[M+NH_4]^+$	$C_{24}H_{26}O_7$	349; 329; 327; 245; 227; 215	6.22 (1H, d, J = 9.47 Hz, 3-H), 7.57 (1H, d, J = 9.62 Hz, 4-H), 7.34 (1H, d, J = 8.61 Hz, 5-H), 6.81 (1H, d, J = 8.67 Hz, 6-H), 5.45 (1H, d, J = 5.06 Hz, 3′-H), **6.69 (1H, d, J = 5.06 Hz, 4′-H)**, 1.45 (3H, s, 5′-CH_3), 1.49 (3H, s, 6′-CH_3), 6.10 (1H, q, J = 6.39 Hz, 3′′-H), 1.82 (3H, s, 5′′-CH_3), 6.00 (1H, q, J = 6.92 Hz, 3′′′-H), 1.85 (3H, s, 5′′′-CH_3)	Praeruptorin B (**8**)
Fr. IX	35.25	467.1444 $[M+K]^+$ 451.1699 $[M+Na]^+$ 446.2321 $[M+NH_4]^+$	$C_{24}H_{28}O_7$	351; 329; 327; 245; 227; 215	6.22 (1H, d, J = 9.37 Hz, 3-H), 7.57 (1H, d, J = 9.38 Hz, 4-H), 7.33 (1H, d, J = 8.45 Hz, 5-H), 6.80 (1H, d, J = 8.44 Hz, 6-H), 5.38 (1H, d, J = 4.98 Hz, 3′-H), 6.61 (1H, d, J = 5.09 Hz, 4′-H), **6.03 (1H, q, J = 6.71 Hz, 3′′′-H)**, 2.00 (3H, d, J = 7.02 Hz, 4′′′-CH_3), 1.88 (3H, s, 5′′′-CH_3)	IAK (**9**)

Table 1 (*continued*)

Source	t_R[a] (min)	MS[1]	Molecular formula	MS[2]	^{1}H-NMR (δ in ppm, J in Hz)[b]	Identity
	35.45	467.1444 $[M+K]^+$ 451.1699 $[M+Na]^+$ 446.2321 $[M+NH_4]^+$	$C_{24}H_{28}O_7$	349; 329; 327; 245; 227; 215	6.22 (1H, d, J = 9.37 Hz, 3-H), 7.57 (1H, d, J = 9.38 Hz, 4-H), 7.33 (1H, d, J = 8.45 Hz, 5-H), 6.80 (1H, d, J = 8.44 Hz, 6-H), 5.38 (1H, d, J = 4.98 Hz, 3′-H), 6.61 (1H, d, J = 5.09 Hz, 4′-H), 1.45 (3H, s, 5′-CH_3), 1.47 (3H, s, 6′-CH_3), **6.13 (1H, q, J = 7.28 Hz, 3′′-H)**, 1.97 (3H, d, J = 6.72 Hz, 4′′-CH_3), 1.86 (3H, s, 5′′-CH_3), 1.19 (6H, d, J = 6.76 Hz, 4′′′,5′′′-CH_3)	PE (**10**)
Fr. X	37.77	469.1467 $[M+K]^+$ 453.1912 $[M+Na]^+$ 448.234 $[M+NH_4]^+$	$C_{24}H_{30}O_7$	351; 329; 245; 227; 215	6.21 (1H, d, J = 9.51 Hz, 3-H), 7.51 (1H, d, J = 9.39 Hz, 4-H), 7.34 (1H, d, J =8.29 Hz, 5-H), 6.80 (1H, d, J = 9.04 Hz, 6-H), **6.55 (1H, d, J =4.93 Hz, 4′-H)**, 1.41 (1H, s, 5′-H), 1.43 (1H, s, 6′-H), 0.98 (2H, d, J = 6.79 Hz, 4′′,5′′-H), 2.33, 2.23 (each 1H, m, 2′′′-H), 2.04 (1H, m, 3′′′-H)	*cis*-3′,4′-*di*-Isovalerylhellactone (**11**)

[a]All retention times were obtained from semi-preparative LC.
[b]The signal in boldface were selected as targeted signals for quantitation.

3.2. *Specific monitoring of regio-isomers*

Although extensive attempts were devoted to the separation of PE and AIK, severe overlap still occurred. Hence, efforts were made towards MRM to offset the resolution between these *regio*-isomers, and another pair of *regio*-isomers, PA *vs*. Pte, was introduced to validate the adaptability of *regio*-specific monitoring through applying exclusive parameters (Fig. 4A).

Diverse ion transition candidates, covering all primary signals in both MS^1 and MS^2 spectra were screened for PA and Pte, and online parameter optimization[26] was carried out for each ion transition candidate. As a result, mild specificity was observed for those candidates being composed of adduct molecular ions (*e.g.* *m/z* 409 $[M + Na]^+$, 404 $[M + NH_4]^+$, and 387 $[M + H]^+$) and grand-daughter ions (*e.g.* *m/z* 245 $[M + H - CH_3COOH - C_4H_6CO]^+$, 227 $[M + H - CH_3COOH - C_4H_7COOH]^+$, and 215 $[M + H - CH_3COOH - C_4H_6CO - CH_2O]^+$) (Fig. 4B–D). Significant selection, nonetheless unsatisfactory, was observed for those candidates consisting of adduct molecular ions (*e.g.*, *m/z* 409, 404, and 387) and daughter ions (*e.g.*, *m/z* 349 $[M + Na - CH_3COOH]^+$, 327 $[M + H - CH_3COOH]^+$, 309 $[M + Na - C_4H_7COOH]^+$, and 287 $[M + H - C_4H_7COOH]^+$) (Fig. 4B–D). Satisfactory specificity was observed, fortunately, for those ion transition candidates composed of daughter ions (*m/z* 349, 327, 309, and 287) and grand-daughter ions (*m/z* 245, 227, and 215) (Fig. 4B–D).

The mass fragmentation pathways of APs are proposed in Supplemental Information Fig. S11. Regarding Pte and PA, the adduct molecular ions underwent step-wise dissociations. The neutral loss of RCOOH from 4′-C dominated the first fragmentation to generate daughter ions at *m/z* 349 and 327 for PA while *m/z* 309 and 287 for Pte, whereas the dissociation of 3′-C–O bond was the inferior pathway to yield daughter ions at *m/z* 309 and 287 for PA while *m/z* 349 and 327 for Pte. Subsequently, identical grand-daughter ions including *m/z* 245, 227, and 215 were observed for either PA or Pte. Because of the distinct mass fragmentation patterns, the ion transition paired by daughter ion and grand-daughter ion could be able to achieve *regio*-specific monitoring for these positional isomers.

Afterwards, the applicability of those rules was assessed for PE and AIK that were almost co-eluted (Fig. 5A). Following extensive assays, some daughter ion > grand-daughter ion pairs such as *m/z* 329 > 245, 329 > 227, 329 > 215, 327 > 245, 327 > 227, and 327 > 215, enabled the *regio*-specific measurements of PE and AIK, and satisfactory discrimination was also achieved with *m/z* 451 > 351, 446 > 329, 451 > 349, and 446 > 327 (Fig. 5B–D). On the contrary, significant overlap occurred when *m/z* 451 > 227 and 451 > 245 were employed (Fig. 5D). Ultimately, *m/z* 329 > 245 and 327 > 245 were involved in the monitoring list of MRM to monitor AIK and PE, respectively, because of their sensitive properties.

3.3. *Extraction of quantitative information for compounds-of-interest*

The quantitative information regarding all compounds-of-interest (**1**–**11**) was extracted from ^{1}H NMR spectra of Frs. III–X. In general, the quantitative signal should show satisfactory response and complete separation from those interfering signals. Obviously, the singlet signal at δ 8.60 yielded by IS1 always served as the qualified reference signal for all

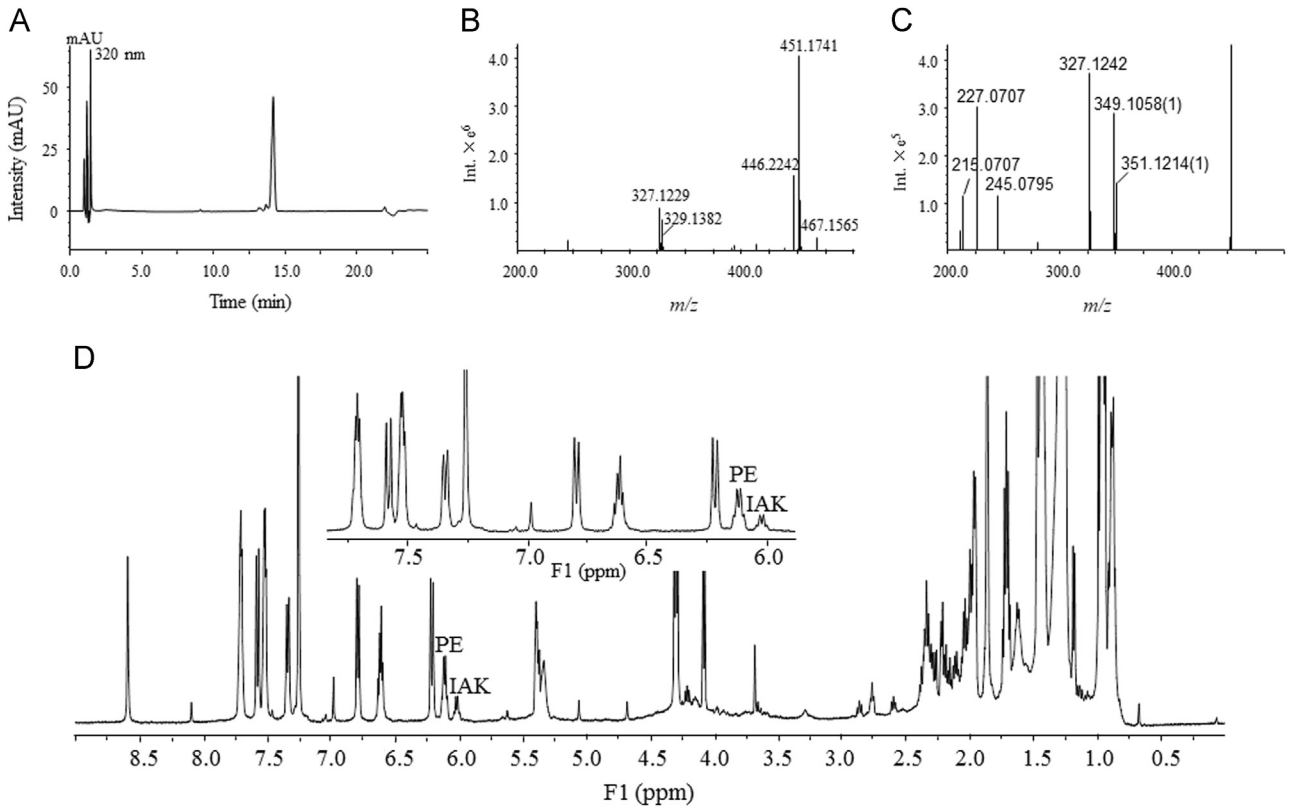

Figure 3 (A) UV (320 nm) chromatogram of Fr. IX. (B) MS^1 spectrum of the primary signal in Fr. IX. (C) MS^2 spectrum of the primary signal in Fr. IX. (D) ^1H NMR ($CDCl_3$, 500 MHz) spectra of Fr. IX in the ranges of δ 0–9.0 and 5.8–7.6. Signal assignments for PE and AIK are also illustrated.

quantitative assays. On the other hand, the signal belonging to 4′-H was demonstrated, fortunately, that it is usually sensitive for the substitutes at 3′-C along with 4′-C and separately distributed in the ^1H NMR spectrum[15]. Therefore, doublet signals belonging to 4′-H (Fig. 2) were usually selected as quantitative signals, such as δ 6.53 for **1** (Supplementary Information Fig. S3), δ 6.63 for **4** (Supplementary Information Fig. S5), δ 6.58 for **5** (Supplementary Information Fig. S6), δ 6.54 for **6** (Supplementary Information Fig. S7), δ 6.69 for **8** (Supplementary Information Fig. S8), and δ 6.55 for **11** (Supplementary Information Fig. S10). It should be mentioned that the left branch of the doublet signal of δ 6.55 was merely employed to provide quantitative information for **11** because significant overlap occurred for the right branch. Regarding PE and IAK, the olefinic proton signals belonging to the angeloyl substitutes at 3′-C and 4′-C for PE (δ 6.13) and IAK (δ 6.03), respectively, exhibited absolute separation and were thereby chosen as the targeted signals (Fig. 2 and Supplementary Information Fig. S9). Despite the absences of 4′-H signals, characteristic singlet signals were observed at δ 5.67 and 5.57 for the protons at 3′-C of **2** and **3**, respectively; hence, these signals were employed for quantitative measurements (Fig. 2). Moreover, the unique doublet signal at δ 8.15 (4-H) was adopted as the diagnostic response for **7** (Fig. 2 and Supplementary Information Fig. S7). As a consequence, the amounts of all eleven analytes in the corresponding fractions were calculated as 0.700, 0.540, 0.060, 1.430, 12.040, 0.150, 1.920, 3.920, 0.804, 3.480, and 1.110 mg for **1**–**11**, respectively.

3.4. *Method validation and simultaneous determination*

Afterwards, Frs. III–X were pooled to generate the pseudo-mixed standard solution that was subsequently used for method validation assays. Following the application of those optimized parameters as well as elution profiles, a representative chromatogram of the calibration sample is shown in Fig. 6A. All compounds-of-interests showed linear properties within respective concentration ranges (Supplemental information Table S2). The results of sensitivity assays (Supplementary Information Table S2), including those lower limits of quantitation (LLOQs, 8.24–184 ng/mL) along with limits of detection (LODs, 0.25–13.4 ng/mL) showed that the method is sensitive enough for simultaneous determination of those eleven coumarins in Peucedani Radix. Moreover, the intra-day (RSDs%, 1.26%–10.22%) and inter-day (RSDs%, 3.67%–13.41%) variations, recovery (79.72%–114.07% with RSDs% among 0.40%–13.82%), and matrix effect assays (97.87%–130.29%, Supplemental Information Table S3) demonstrated that the developed method could meet the requirements of reliable quantitation.

The validated method was then implemented for simultaneous determination of eleven coumarins (**1**–**11**) in eleven batches of Peucedani Radix (PR1–PR11). In particular, two positional isomers, *i.e.* PA *vs.* Pte and PE *vs.* IAK, were presented. The typical chromatogram of Peucedani Radix is exhibited in Fig. 6B following measurement in parallel with those calibration samples, and the quantitative results are summarized in Table 2. Overall, significant variations regarding the quantitative profiles were observed among the crude materials. The contents of four batches (PR1, PR3, PR9 and PR10) were outliers from the profile cluster

Table 2 The contents (μg/100 mg) of eleven analytes in the eleven batches of Peucedani Radix (PR1–11).

No.	Content										
	1	**2**	**3**	**4**	**5**	**6**	**7**	**8**	**9**	**10**	**11**
PR1	0.46 ± 0.03	468.49 ± 42.94	4.89 ± 0.13	11.01 ± 0.95	1279.74 ± 42.82	5.14 ± 0.20	6.09 ± 0.32	1409.43 ± 61.12	283.08 ± 12.98	85.49 ± 3.60	318.01 ± 10.35
PR2	273.05 ± 12.16	273.31 ± 10.92	25.95 ± 0.51	54.13 ± 1.48	571.79 ± 31.28	5235.87 ± 252.25	690.44 ± 5.62	1687.03 ± 177.01	421.89 ± 9.16	1769.13 ± 82.70	537.62 ± 12.21
PR3	145.48 ± 5.57	101.58 ± 3.70	8.21 ± 0.32	638.55 ± 19.69	1954.78 ± 16.56	2070.15 ± 50.38	380.94 ± 29.54	846.10 ± 0.06	138.72 ± 3.09	689.61 ± 25.27	217.23 ± 6.21
PR4	158.22 ± 14.97	217.79 ± 3.48	26.78 ± 0.96	51.27 ± 3.34	357.13 ± 34.80	5302.49 ± 168.16	771.17 ± 52.06	1691.26 ± 76.10	404.20 ± 26.84	1853.48 ± 93.15	586.09 ± 28.88
PR5	143.58 ± 6.10	257.32 ± 16.16	33.67 ± 1.65	50.56 ± 5.02	249.59 ± 4.68	6009.39 ± 92.16	903.01 ± 68.28	1275.93 ± 94.67	231.21 ± 8.39	2053.74 ± 36.62	573.50 ± 13.76
PR6	199.52 ± 6.33	157.22 ± 6.96	6.44 ± 0.13	48.31 ± 2.45	541.90 ± 13.33	5309.92 ± 150.23	699.92 ± 49.66	1574.89 ± 113.24	318.44 ± 17.50	1681.30 ± 90.76	526.74 ± 10.56
PR7	301.41 ± 15.21	174.36 ± 7.87	12.55 ± 0.38	60.39 ± 1.53	403.20 ± 16.77	5180.24 ± 207.37	782.22 ± 32.70	1279.78 ± 0.08	279.61 ± 6.49	1557.53 ± 53.09	457.16 ± 28.91
PR8	216.65 ± 4.51	117.88 ± 9.78	11.75 ± 0.38	216.65 ± 19.43	1073.94 ± 97.90	2880.66 ± 238.03	570.82 ± 74.75	1154.92 ± 0.06	255.54 ± 21.17	1014.20 ± 76.02	317.93 ± 35.54
PR9	8.98 ± 0.08	410.73 ± 38.33	5.24 ± 0.23	42.21 ± 1.13	1027.48 ± 11.26	232.71 ± 2.19	19.37 ± 0.10	1022.17 ± 13.99	133.68 ± 11.38	74.07 ± 7.18	230.98 ± 15.89
PR10	51.60 ± 5.77	47.09 ± 3.59	5.67 ± 0.14	520.01 ± 35.67	2292.31 ± 22.51	2594.77 ± 49.71	420.06 ± 36.30	337.68 ± 0.08	62.08 ± 3.26	1166.05 ± 36.47	297.28 ± 25.98
PR11	156.09 ± 13.78	145.16 ± 11.25	13.48 ± 0.62	37.78 ± 3.94	318.15 ± 30.93	2115.73 ± 33.75	485.19 ± 50.62	1000.20 ± 2.81	202.62 ± 21.65	823.23 ± 22.50	272.82 ± 13.50

consisting of the other batches after the preliminary hierarchical cluster analysis (data now shown), agreeing well with the findings archived in our previous article[14]. Except for PR1 (5.14 μg/100 mg) and PR9 (232.71 μg/100 mg), PA was always observed as the most abundant component in Peucedani Radix (2070.15–6009.39 μg/100 mg). Most batches were also rich in compound **8** (337.68–1691.26 μg/100 mg) together with PE (74.07–2053.74 μg/100 mg). On the other hand, minor occurrences were detected, in most cases, for compound **3** (4.89–33.67 μg/100 mg). As expected, the ratio of each analyte, except PE and IAK, between the absolute contents obtained here and those quasi-contents in Ref. 14 were very similar across among different batches (PR1–PR11). It is also worth mentioning that both PE and IAK were grouped into a single compound namely PE in our previous article due to the extensive overlapping signals as well as nonspecific ion transition; however, the sum of the absolute contents of PE and IAK showed identical variation tendency with the quasi-content of PE[14] amongst all batches.

Although LC has been widely claimed as an efficient separation tool (especially when using sub-micron chromatographic particles), it cannot fully meet the chromatographic separation demands for TCMs. Therefore, additional efforts by analytical scientists are required to search an orthogonal means to enhance the chromatographic potential of LC. Ion mobility mass spectrometry (IM-MS) has been most frequently mentioned as a qualified choice, in particular for discriminating those isomers, because each component usually owns unique collision cross section in the ion mobility chamber[29]. However, we suggested that MRM might exhibit the potential to discriminant isomers because different tandem mass spectrometric behaviors always occur between isomers. In current study, specific monitoring was achieved for those positional isomers, *e.g.* Pte *vs.* PA[14] and PE *vs.* IAK, following careful parameter optimization. Hence, MRM might be able to replace the role of IM-MS, to some extent, by serving as a complementary separation dimension for LC.

We previously proposed a protocol[14] for large-scale relative quantitation of complicated matrices which could fulfill the demands of comparative metabolomics. However, absolute contents of metabolites, as many as possible, are of great importance for clinical diagnosis and personalized medicine. Fortunately, the current strategy meets these goals because it provides a flexible procedure to identify and quantify ten analytes from a TCM extract in an authentic compound-independent manner. In addition, it is convenient to accumulate metabolites-of-interest *via* scheduling valve-switching program for the home-made fraction collection module. As a consequence, the combination of the current study and the previous one[14] might offer a fit-for-purpose tool to completely reveal the quantitative metabolome of TCMs.

4. Conclusions

In the current study, offline LC–NMR–MS/MS was applied as the core idea for a new three-step strategy for multi-component targeted quantitation of Peucedani Radix without the use of authentic compounds as external standards. First, UMS was fragmented into ten fractions (Frs. I–X) with a home-made automated fraction collection module. Secondly, definite structural information and quantitative properties regarding compounds-of-interest were obtained by assaying each fraction with LC–IT-TOF-MS and NMR spectroscopy in parallel. Thirdly, those well-characterized fractions (Frs. III–X) were

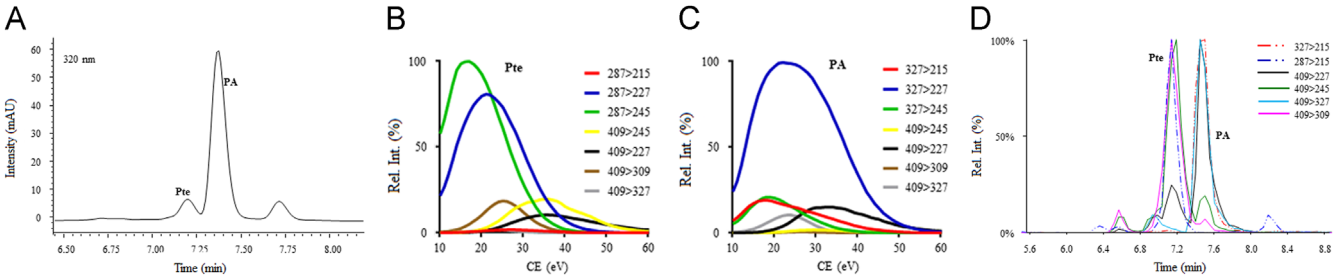

Figure 4 (A) UV (320 nm) chromatogram of UMS among 6.45–8.25 min, showing that absolute separation is accomplished between PA and Pte. (B) Relative intensity-CE curves of Pte, corresponding to different ion transition candidates (*m/z* 287 > 215, 287 > 227, 287 > 245, 409 > 245, 409 > 227, 409 > 309, and 409 > 327). (C) Relative intensity-CE curves of PA, corresponding to different ion transition candidates (*m/z* 327 > 215, 327 > 227, 327 > 245, 409 > 245, 409 > 227, 409 > 309, and 409 > 327). (D) Overlaid extracted ion current (XIC) chromatogram of *m/z* 327 > 215, 287 > 215, 409 > 227, 409 > 245, 409 > 327, and 409 > 309 for UMS among 5.60–8.80 min, indicating that *regio*-specific monitoring can be accomplished with *m/z* 327 > 215 and 287 > 215 instead of *m/z* 409 > 227, 409 > 245, 409 > 327, and 409 > 309.

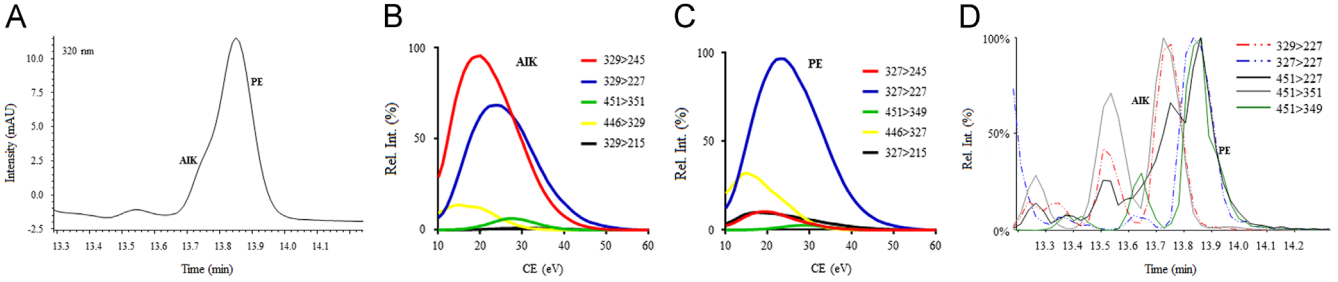

Figure 5 (A) UV (320 nm) chromatogram of UMS among 13.30–14.15 min, showing that overlapping signals occurs between AIK and PE. (B) Relative intensity-CE curves of AIK, corresponding to different ion transition candidates (*m/z* 329 > 245, 329 > 227, 451 > 351, 446 > 329, and 329 > 215). (C) Relative intensity-CE curves of PE, corresponding to different ion transition candidates (*m/z* 327 > 245, 327 > 227, 451 > 349, 446 > 327, and 327 > 215). (D) Overlaid XIC chromatogram of *m/z* 329 > 227, 327 > 227, 451 > 227, 451 > 351, and 451 > 349 for UMS among 13.20–14.30 min, indicating that *regio*-specific monitoring can be achieved unless the employment of *m/z* 451 > 227.

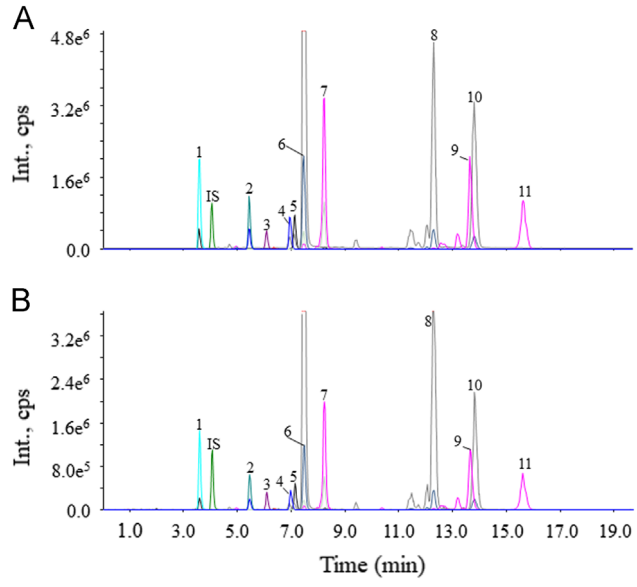

Figure 6 Representative overlaid extracted ion current (XIC) chromatograms of the pseudo-mixed standard solution containing **1**–**11** (A) and Peucedani Radix extract (B).

pooled to generate the pseudo-mixed standard solution which was further implemented for simultaneous determination of eleven primary coumarins (**1**–**11**) in Peucedani Radix by LC–MRM. In particular, exclusive monitoring of *regio*-isomers was achieved for Pte *vs.* PA as well as PE *vs.* IAK by online optimizing specific parameters. Diverse validation assays demonstrated the reliability of the quantitative results, and significant variations occurred among different batches; PA, praeruptorin B, and PE usually showed abundant distributions in most cases. Above all, the new procedure enables authentic compound-free determination of the primary components in Peucedani Radix. This approach can be applied as a practical tool for the quantitative evaluation of TCMs.

Acknowledgments

This work was financially supported by National Science Fund of China (Nos. 81773875, 81403073 and 81530097), Quality Guarantee System of Chinese Herbal Medicines (No. 201507002), foundation from Beijing University of Chinese Medicine (No. 2016-JYB-XJQ004), and the Macao Science and Technology Development Fund (007/2014/AMJ).

Appendix A. Supporting information

Supplementary data associated with this article can be found in the online version at https://doi.org/10.1016/j.apsb.2018.01.005.

References

1. Zhang A, Sun H, Wang X. Mass spectrometry-driven drug discovery for development of herbal medicine. *Mass Spectrom Rev* 2016. Available from :<http://dx.doi.org/10.1002/mas.21529>.
2. Liang QL, Liang XP, Wang YM, Xie YY, Zhang RL, Chen X, et al. Effective components screening and anti-myocardial infarction mechanism study of the Chinese medicine NSLF6 based on "system to system" mode. *J Transl Med* 2012;**10**:26.
3. Xue T, Roy R. Studying traditional Chinese medicine. *Science* 2003;**300**:740–1.
4. Jiang Y, David B, Tu P, Barbin Y. Recent analytical approaches in quality control of traditional Chinese medicines–a review. *Anal Chim Acta* 2010;**657**:9–18.
5. Li P, Qi LW, Liu EH, Zhou JL, Wen XD. Analysis of Chinese herbal medicines with holistic approaches and integrated evaluation models. *Trac Trend Anal Chem* 2008;**27**:66–77.
6. Li DW, Zhu M, Shao YD, Shen Z, Weng CC, Yan WD. Determination and quality evaluation of green tea extracts through qualitative and quantitative analysis of multi-components by single marker (QAMS). *Food Chem* 2016;**197 Pt B**:1112–20.
7. Gao XY, Jiang Y, Lu JQ, Tu PF. One single standard substance for the determination of multiple anthraquinone derivatives in rhubarb using high-performance liquid chromatography-diode array detection. *J Chromatogr A* 2009;**1216**:2118–23.
8. Wang W, Ma X, Guo X, Zhao M, Tu P, Jiang Y. A series of strategies for solving the shortage of reference standards for multi-components determination of traditional Chinese medicine, Mahoniae Caulis as a case. *J Chromatogr A* 2015;**1412**:100–11.
9. Zou P, Song Y, Lei W, Li J, Tu P, Jiang Y. Application of ^{1}H NMR-based metabolomics for discrimination of different parts and development of a new processing workflow for *Cistanche deserticola*. *Acta Pharm Sin B* 2017;**7**:647–56.
10. Wishart DS, Jewison T, Guo AC, Wilson M, Knox C, Liu Y, et al. HMDB 3.0—the human metabolome database in 2013. *Nucleic Acids Res* 2013;**41**:D801–7.
11. Bingol K, Li DW, Zhang B, Bruschweiler R. Comprehensive metabolite identification strategy using multiple two-dimensional NMR spectra of a complex mixture implemented in the COLMARm Web server. *Anal Chem* 2016;**88**:12411–8.
12. Chinese Pharmacopoeia Commission. *Pharmacopoeia of the People's Republic of China*, Vol I. Beijing: China Medical Science Press 2015; p.265.
13. Song Y, Jing W, Yan R, Wang Y. Research progress of the studies on the roots of *Peucedanum praeruptorum* Dunn (Peucedani Radix). *Pak J Pharm Sci* 2015;**28**:71–81.
14. Song Y, Song Q, Liu Y, Li J, Wan JB, Wang Y, et al. Integrated workflow for quantitative metabolome profiling of plants, Peucedani Radix as a case. *Anal Chim Acta* 2017;**953**:40–7.
15. Song YL, Jing WH, Chen YG, Yuan YF, Yan R, Wang YT. ^{1}H nuclear magnetic resonance based-metabolomic characterization of Peucedani Radix and simultaneous determination of praeruptorin A and praeruptorin B. *J Pharm Biomed Anal* 2014;**93**:86–94.
16. Song YL, Jing WH, Du G, Yang FQ, Yan R, Wang YT. Qualitative analysis and enantiospecific determination of angular-type pyranocoumarins in Peucedani Radix using achiral and chiral liquid chromatography coupled with tandem mass spectrometry. *J Chromatogr A* 2014;**1338**:24–37.
17. Song YL, Jing WH, Yan R, Wang YT. Enantiomeric separation of angular-type pyranocoumarins from Peucedani Radix using AD-RH chiral column. *Nat Prod Res* 2014;**28**:545–50.
18. Song YL, Zhang QW, Li YP, Yan R, Wang YT. Enantioseparation and absolute configuration determination of angular-type pyranocoumarins from peucedani radix using enzymatic hydrolysis and chiral HPLC–MS/MS analysis. *Molecules* 2012;**17**:4236–51.
19. Chang HM, But PPH, Yao SC, Wang LL, Yeung SCS. *Pharmacology and Applications of Chinese Materia Medica*, Vol. *2*. Singapore: World Scientific Publisher 2001. p.905.
20. Zhao NC, Jin WB, Zhang XH, Guan FL, Sun YB, Adachi H, et al. Relazant effects of pyranocoumarin compounds isolated from a Chinese medical plant, Bai-Hua Qian-Hu, on isolated rabbit tracheas and pulmonary arteries. *Biol Pharm Bull* 1999;**22**:984–7.
21. Chang TH, Adachi H, Okuyama T, Zhang KY. Effects of 3′-angeloyloxy-4′-acetoxy-3′,4′-dihydroseselin on myocardial dysfunction after a brief ischemia in anesthetized dogs. *Acta Pharmacol Sin* 1994;**15**:388–91.
22. Hong MJ, Kim J. Determination of the absolute configuration of khellactone esters from *Peucedanum japonicum* Roots. *J Nat Prod* 2017;**80**:1354–60.
23. Liu R, Feng L, Sun A, Kong L. Preparative isolation and purification of coumarins from *Peucedanum praeruptorum* Dunn by high-speed counter-current chromatography. *J Chromatogr A* 2004;**1057**:89–94.
24. Hou Z, Xu D, Yao S, Luo J, Kong L. An application of high-speed counter-current chromatography coupled with electrospray ionization mass spectrometry for separation and online identification of coumarins from *Peucedanum praeruptorum* Dunn. *J Chromatogr B* 2009;**877**:2571–8.
25. Sun YF. Isolation and identification of chemical constituents from an alcoholic extract of *Notopterygium incisium*. *Bull Chin Mater Med* 1985;**10**:31–3.
26. Song Y, Song Q, Li J, Zheng J, Li C, Zhang Y, et al. An integrated platform for directly widely-targeted quantitative analysis of feces part II: an application for steroids, eicosanoids, and porphyrins profiling. *J Chromatogr A* 2016;**1460**:74–83.
27. Chen YG, Song YL, Wang Y, Yuan YF, Huang XJ, Ye WC, et al. Metabolic differentiations of *Pueraria lobata* and *Pueraria thomsonii* using ^{1}H NMR spectroscopy and multivariate statistical analysis. *J Pharm Biomed Anal* 2014;**93**:51–8.
28. Tao Y, Luo J, Lu Y, Xu D, Hou Z, Kong L. Rapid identification of two species of *Peucedanum* by high-performance liquid chromatography-diode array detection-electrospray ionization tandem mass spectrometry. *Nat Prod Commun* 2009;**4**:1079–84.
29. Zhou Z, Shen X, Tu J, Zhu ZJ. Large-scale prediction of collision cross-section values for metabolites in ion mobility-mass spectrometry. *Anal Chem* 2016;**88**:11084–91.